STRUCTURAL ORGANIZATION OF A MAMMALIAN CELL

All eukaryotic cells present qualitatively a similar structural organization that can vary quantitatively depending on their degree of differentiation and specialization as well as functional state. The electron micrograph shows at low magnification highly specialized acinar cells of rat pancreas, which represent the prototype of a polarized exocrine secretory cell. Several such acinar cells form a functional unit, named the secretory acinus.

Each cell consists of two major compartments, the nucleus and the cytoplasm, and these are the focus of the first chapter. The cytoplasm of different cell types contains a common set of membrane-bound organelles and the various structural components of the cytoskeleton. They are both embedded in the cytosol, which houses the intermediate metabolism and is the location where protein synthesis commences and proteasomal degradation of (misfolded) proteins as well as protein *O*-GlcNAcylation occur. The rough endoplasmic reticulum (RER) is involved in translocation of secretory and membrane proteins and protein quality control, is the site of initiation of protein *N*-glycosylation, and is a major Ca^{2+} store. Lipids are also synthesized in the endoplasmic reticulum. Many proteins and lipids are transported to the Golgi apparatus, where they receive different post-translational modifications and are sorted to their final destinations. The protein polypeptide:GalNAc *O*-glycosylation is initiated in the Golgi apparatus. The pre-Golgi intermediates are implicated in anterograde and retrograde transport of cargo between the endoplasmic reticulum and the Golgi apparatus. In acinar pancreatic cells and other types of secretory cells, secretory proteins are sorted and packed into immature secretory granules, so-called condensing vacuoles (CV) forming in the *trans* Golgi apparatus. They mature into zymogen granules (ZG), which are stored in the apical cytoplasm and undergo secretion on stimulation. The endoplasmic reticulum and its transitional elements, the pre-Golgi intermediates, the Golgi apparatus, and secretory granules constitute the secretory pathway. Further cellular organelles are the mitochondria (M), which mostly generate energy; peroxisomes, which perform oxidative reactions; lysosomes and autophagosomes/autolysosomes, which have degradative functions; and endosomes, which are involved in cellular uptake of extracellular substances.

The plasma membrane is the cell's boundary with its environment. In epithelial cells such as the acinar cells, two plasma membrane domains can be distinguished. The apical plasma membrane domain forms the acinar lumen (AL) and is separated by junctional complexes (arrows) from the lateral (LPM) and basal (BPM) plasma membrane domain.

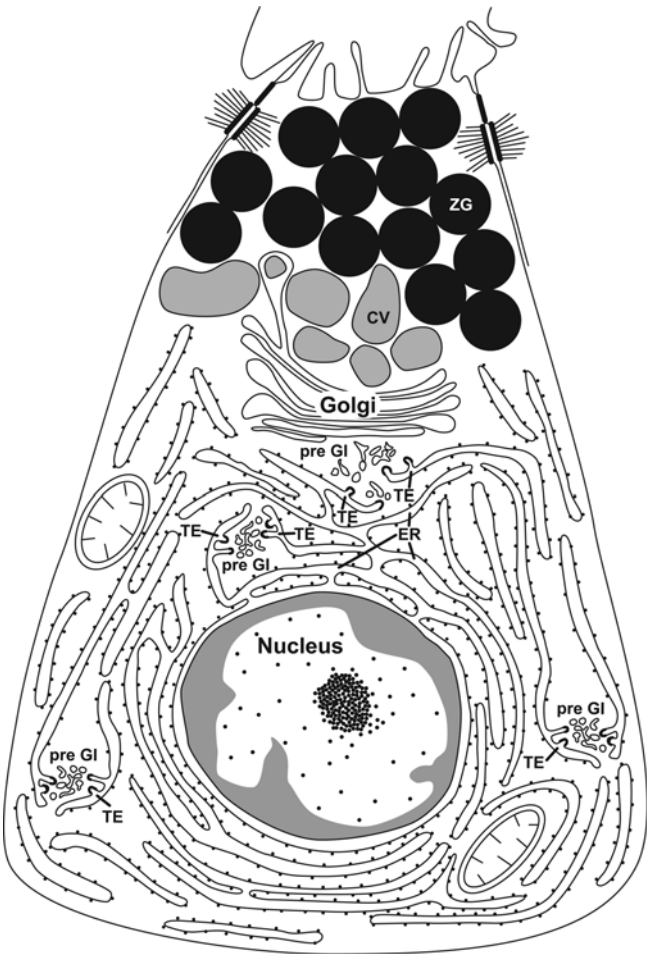

The diagram presents a simplified version of a pancreatic acinar cell.

Magnification: ×11,250

M. Pavelka, J. Roth, *Functional Ultrastructure: Atlas of Tissue Biology and Pathology*, Third Edition,
DOI 10.1007/978-3-7091-1830-6_1, © Springer-Verlag Vienna 2015

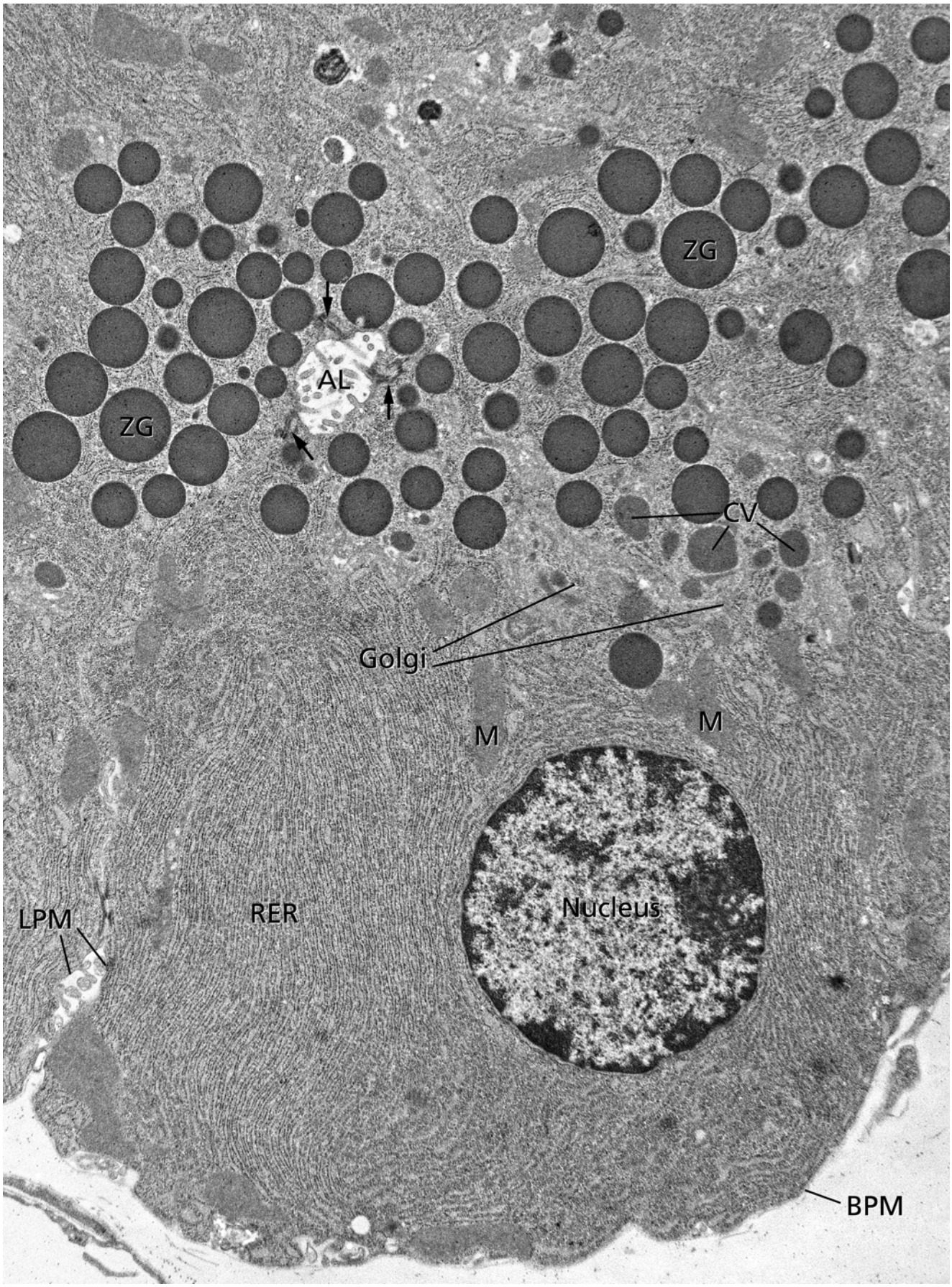
ZG
AL
ZG
CV
Golgi
M
M
Nucleus
LPM
RER
BPM

CELLULAR FINE STRUCTURES AND ARCHITECTURES VISUALIZED THREE-DIMENSIONALLY BY USING FIB-SEM TOMOGRAPHY

Focused ion beam–scanning electron microscopy tomography (FIB-SEM tomography; also called "slice and view") is a novel approach for three-dimensional imaging of biological samples. In using this procedure, a sample is repeatedly milled with the focused ion beam (FIB), and each newly produced block face is imaged with the scanning electron microscope (SEM). This process can be repeated ad libitum in arbitrarily small increments allowing 3D analysis of relatively large volumes such as eukaryotic cells. The method works particularly well with plastic embedded material as prepared for thin section transmission electron microscopy.

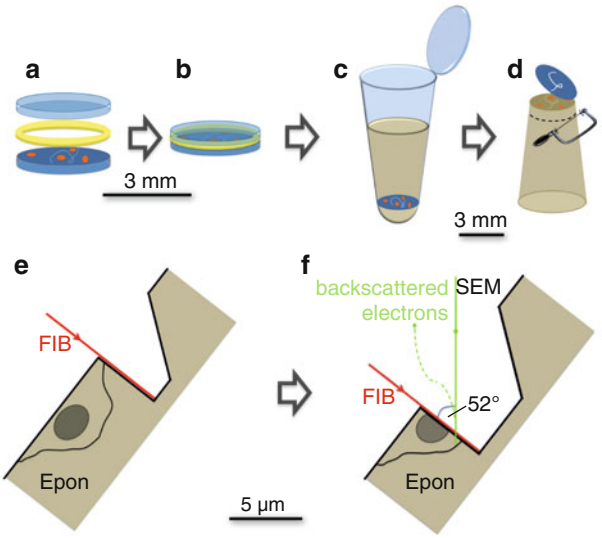

The diagram explains the sample preparation and imaging protocol. Cells of a human pancreatic carcinoid cell line (BON cells) were grown on sapphire discs. A sandwich of two discs and a gold ring as spacer (a and b) is then high-pressure frozen, opened, freeze substituted, and embedded in Epon (c). The sapphire disc is then removed, so that the cells remain at the surface of the Epon block (d). The Epon block is sawed with a jigsaw to a height of about 1 mm and mounted on an SEM specimen stub. Pictures e and f show the process of "slice and view" as performed in a FIB-SEM (simplified diagram). Firstly, a block face is exposed by milling a cross section into the Epon block with the FIB (e). A small amount of the Epon is then removed with the FIB and the newly occurring block face is imaged with the SEM using, in this case, the backscattered electron signal (f). This process can be repeated ad libitum to obtain a tomographic dataset.

The figure represents a dataset of a volume of $X = 28$ µm, $Y = 19$ µm, and $Z = 6.5$ µm. Panel A is a representation of the dataset obtained with the IMOD software showing the *XY*, *XZ* and the *YZ* plane. Because of the minute slicing thickness (10 nm) in the range of the image pixel size (12.5 nm), an almost isotropic resolution is obtained. For this dataset, the slice and view process was performed in two steps. In a first step, a depth of 3 µm was milled and imaged in *Z* direction. After bringing the area of interest back into the image center and readjusting focus, brightness, and contrast, a second slice and view process imaged a depth of another 3.5 µm. Redeposition of material on the block face has to be removed after acquisition of the first dataset, resulting in the loss of a few slices between the two datasets. For this reason, the second dataset does not align perfectly with the first, which results in the line visible at $Z = 3$ µm in the *XZ* and *YZ* plane.

The ultrastructure of the cell is well retained and, as can be seen in the higher magnification in panels B–E, the shape of organelles – such as the microtubule organizing center (panel B; MTOC), the Golgi-apparatus (G in panel C), and chromogranin A containing vesicles (arrows in B and C) – can be clearly observed. The two images in D and E show two successive sections of the same mitochondrion to illustrate the high resolution in Z direction. In panel E, the interconnection between the two parts of the mitochondrion becomes visible (arrowheads). Panel F is a visualization of the same dataset using the AVIZO software, highlighting the complex structure of the apical cell surface and the cell nuclei. Because of the big difference in brightness between cytoplasm and extracellular space, it was possible to perform a semiautomatic segmentation of the cell membrane (light blue). The surface of the three nuclei was segmented manually.

Figure and diagram are modified from Villinger et al. (2012) Histochem Cell Biol 138: 549

References

Villinger C, Gregorius H, Kranz Ch, Höhn K, Münzberg C, von Wichert G, Mizaikoff B, Wanner G, Walther P (2012) FIB/SEM-tomography with TEM-like resolution for 3D imaging of high pressure frozen cells. Histochem Cell Biol 138:549

Villinger C, Schauflinger M, Gregorius H, Kranz C, Höhn K, Nafeey S, Walther P (2014) Three-dimensional imaging of adherent cells using FIB/SEM and STEM. Methods Mol Biol 2014:1117

Wanner G, Schäfer T, Lütz-Meindl U (2013) 3-D analysis of dictyosomes and multivesicular bodies in the green alga Micrasterias denticulata by FIB/SEM tomography. J Struct Biol 184:203

Magnification: ×4,875 (**A**), ×14,500 (**B**–**E**), ×4,820 (**F**)

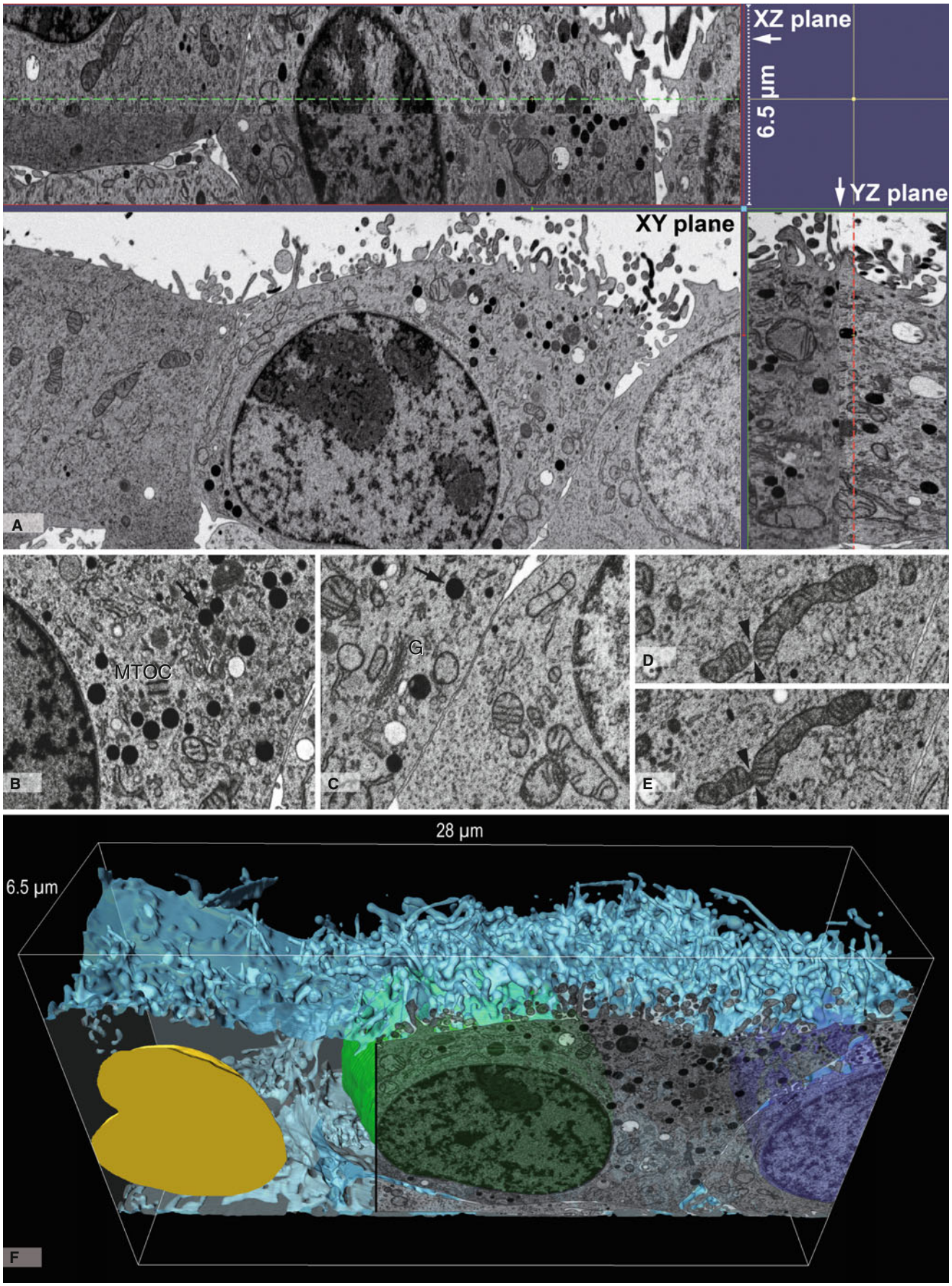
XZ plane
6.5 µm
YZ plane
XY plane
A
MTOC
B
G
C
D
E
28 µm
6.5 µm
F